

# Electronic and magnetic properties of the Co/Fe(001) interface and the role of oxygen

L. Duò, R. Bertacco, G. Isella, and F. Ciccacci

*INFN–Dipartimento di Fisica, Politecnico di Milano, piazza Leonardo da Vinci 32, 20133 Milano, Italy*

M. Richter

*Department of Theoretical Solid State Physics, IFW Dresden e. V., P.O. Box 270016, D-01171 Dresden, Germany*

(Received 15 December 1999)

A combined theoretical and experimental study of the structural, electronic, and magnetic properties of a Co thin film growth onto Fe(001) substrate is reported. This includes also an analysis of the role of oxygen in modifying the properties of the Co/Fe interaction. Experimental results obtained by spin-resolved absorbed current and inverse photoemission spectroscopies, as probes of the empty electron states, show nice agreement with first-principles full-potential local-orbital calculations. Co growth has been shown to display different paths according to various conditions. The Co/Fe(001) interface shows a distorted cubic Co growth (known as bct) up to about 15 monolayers (ML) turning to the equilibrium hcp Co structure for larger thickness. Co growth onto the surface oxidized Fe(001)- $p(1 \times 1)$ O shows a similar behavior with an extended stability range of the bct structure up to about 35 ML. Spin-dependent effects are, moreover, enhanced due to an oxygen surfactant action. FeCo(001) formation is shown to take place by thermal treatment of the interface. Its features are interpreted in terms of band filling arguments, and the surface oxidation displays again a considerable enhancement of spin-dependent effects in analogy with the surface oxidation of pure Fe(001).

## I. INTRODUCTION

Molecular beam growth of thin films under ultrahigh vacuum (UHV) conditions is an important technique for the creation of new phases of solids, which can give rise to epitaxially stabilized materials showing metastable crystal structures. The strong link between structural and electronic properties is particularly relevant when magnetic species are involved, as substrates and/or thin film overlayers, in the growth of interfaces or multilayers since these aspects may strongly influence their magnetic properties. Due to the great interest, both from fundamental and technological points of view, these systems are being extensively investigated.<sup>1</sup> In particular, concerning Co, which has a hcp equilibrium structure, it has been found that it is possible to crystallize thin films in cubic metastable phases such as the bcc on GaAs and Fe (Ref. 2) and the fcc on Cu (Refs. 3 and 4) substrates.

In the following we focus our attention on the electronic and magnetic properties vs crystal structure of the Co/Fe(001) interface which allows a variety of different growing regimes (i.e., cubic and hexagonal).<sup>3,5,6</sup> We also show that when the interface is thermally treated the formation of a stoichiometric FeCo compound takes place, with a CsCl structure. Moreover, the role of oxygen may also be relevant in modifying the properties of the Co/Fe(001) interface growth. In the case of the Fe(001) surface, a controlled exposure to oxygen induces a structural modification, resulting in a well-ordered Fe(001)- $p(1 \times 1)$ O surface.<sup>7-9</sup> It has been recently evidenced<sup>10</sup> that the atomic configuration of the surface Fe atoms interacting with oxygen strongly enhances the spin-dependent effects showing a larger exchange splitting between opposite spin levels. Moreover, this surface oxygen acts as a surfactant in room-temperature Fe homoepitaxy, improving considerably the surface order and enhancing the magnetic properties of the topmost Fe layers.<sup>11</sup> By analogy,

similar oxygen-induced effects are worth searching for also on the Co/Fe(001) interface since they might occur upon the surface oxidation of FeCo and the Co epitaxy on Fe(001)- $p(1 \times 1)$ O, respectively.

In this paper we report a combined experimental and theoretical study on the above issues. Results obtained by means of empty states spectroscopies, namely, absorbed current (AC) and inverse photoemission (IPE) spectroscopies both performed in the spin-resolved mode, are compared to first-principles spin-projected calculations based on a full-potential nonorthogonal local-orbital (FPLO) minimum basis band-structure scheme.<sup>12</sup> The discussion is basically performed along three topics related to (a) the Co/Fe(001) interface formation at room temperature and the analysis of the spin-dependent effects related to the cubic-to-hexagonal phase transition, (b) the Co growth onto the Fe(001)- $p(1 \times 1)$ O surface and the comparison of its features with respect to the Co/Fe(001) growth, and (c) the formation and magnetic properties of the FeCo compound and of its surface oxidation.

## II. EXPERIMENTAL AND THEORETICAL DETAILS

The experiments herein reported are spin-resolved AC and IPE, performed in an UHV system (base pressure  $< 7 \times 10^{-11}$  mbar) equipped with standard surface characterization techniques.<sup>13</sup> The Fe(001) sample is obtained by growing a 300-nm-thick Fe film onto a MgO(001) substrate in UHV conditions. After annealing at 850 K, a clean and ordered Fe(001) surface is obtained as evidenced by x-ray photoemission spectroscopy (XPS) and low-energy electron diffraction (LEED) analysis.<sup>14</sup> Fe(001)- $p(1 \times 1)$ O is obtained by exposing the clean Fe(001) surface to 30 L

(1 L =  $1 \times 10^{-6}$  Torr s) of  $O_2$  at 450 K and then flash heating at 900 K for few seconds.<sup>15</sup> This procedure gives a nicely ordered structure, as evidence by the sharp  $p(1 \times 1)$  LEED pattern. XPS analysis for the determination of the core level intensities is also in good agreement with previous data on the Fe(001)- $p(1 \times 1)$ O surface.<sup>16</sup>

The growth of Co overlayers has been carried out onto Fe(001) and Fe(001)- $p(1 \times 1)$ O, at a pressure of  $\sim 5 \times 10^{-10}$  mbar, by thermal evaporation from a water-cooled electron bombardment cell. The deposition has been performed, keeping the samples at room temperature, at a rate of  $\sim 8 \text{ \AA}/\text{min}$  as measured by a calibrated quartz microbalance. In the following we will report Co coverages in monolayers (ML), the thickness of 1 ML corresponding conventionally to the Fe(001) substrate spacing, namely, 1.43  $\text{Å}$ . The film purity was checked by XPS, which also allowed us to obtain estimations of the Co thickness in good agreement with our deposition rates.

Samples have been magnetized in the plane along the [100] direction of the Fe lattice, then spectra taken in magnetic remanence, as usual in electron spectroscopies. Measurements have been performed at room temperature. The collimated and transversely polarized electron beam impinging on the samples is produced by a spin-resolved electron gun based on a negative electron affinity GaAs photocathode.<sup>13</sup> Absolute calibration of the beam polarization ( $P_0$ ) was performed in a separate experiment by Mott scattering,<sup>17</sup> yielding a value  $P_0 = (25 \pm 2)\%$ . The IPE spectra are taken in the isochromat mode by collecting photons at a fixed energy  $h\nu = (9.4 \pm 0.3) \text{ eV}$  while varying the incident beam energy.<sup>13</sup> The AC spectra are recorded by measuring the target electron current running to ground. Data are normalized to the current impinging onto the sample. All spectra reported have been collected at normal incidence with the beam polarization either parallel or antiparallel to the sample magnetization.

First-principles band-structure calculations optimized to obtain reliable eigenvalues for empty states up to about 20 eV above the Fermi level ( $E_F$ ) have been performed by the FPLO scheme.<sup>12</sup> In this scheme the crystal potential and density are represented as a lattice sum of local overlapping nonspherical contributions. The decomposition of the exchange and correlation potential into local parts is done using a technique of partitioning of unity, resulting in local shape functions, which add exactly to unity in the whole crystal and which are easily treated numerically. The method is all electron, which means that core relaxation is properly taken into account. The calculations were carried out in a scalar-relativistic approximation using an updated version<sup>18</sup> of the code published in Ref. 12. Though the scheme is designed as a minimum basis method, it allows one to include unoccupied atomiclike orbitals into the valence basis. This possibility was utilized in the present calculations by using a  $3d/4s/4p/4d$  atomiclike orbital basis. This choice gives a reasonably complete basis set for the description of unoccupied valence states in the region 0–20 eV above  $E_F$ .

To interpret the data reported below, we performed these calculations for bcc Fe and for Co in different structures, namely, bcc, tetragonally distorted bcc (known as bct), and hcp. Due to the scattering geometry, the accessible states lie along the  $\Gamma H$  direction of the bulk Brillouin zone (BZ) for

the cubic and tetragonal structures having a surface on the (001) plane and along  $\Gamma M$  for the hexagonal one which has a  $(11\bar{2}0)$  surface orientation, as indicated below. Calculations have been performed for the FeCo compound as well; they will be further discussed in Sec. V. The normal incidence geometry gives also a further symmetry constraint on the states which can be occupied in the solid by the incoming electrons. They are described by free electron bands outside the solid and belong to the  $\Delta_1$  symmetry of the bcc or bct lattice: therefore, such states are those directly probed by AC spectroscopy.<sup>19,20</sup> In the subsequent radiative decay to the lower-lying empty states, dipole selection rules allow only for given transitions selecting the symmetry of the final states. For the bcc or bct BZ, these are the  $\Delta_1$  and  $\Delta_5$  bands which are probed by IPE spectroscopy. If we translate the notation into a spherical harmonics language, we can assume that the states accessible to AC spectroscopy have  $m_l = 0$ ; via the dipole selection rule concerning  $m_l$ , IPE final states are represented by wave functions with  $m_l = 0, \pm 1$  symmetry. Moreover, it has to be noted that all IPE data refer to the photons taken off unpolarized at  $45^\circ$  from the sample normal. Consequently, the electric field component parallel to the surface, which refers to  $m_l = \pm 1$  final states, has a 3 times higher detection probability than the perpendicular component, which refers to  $m_l = 0$  final states.<sup>19</sup> This will generally make very weak the IPE signal connected to final states having  $m_l = 0$  symmetry.

### III. Co ON Fe(001)

Co/Fe(001) thin films up to  $\sim 15$  ML are known to grow in a metastable distorted bcc structure, known as body-centered tetragonal (bct), and to display a phase transition, turning to the hcp structure with the  $(11\bar{2}0)$  orientation, for larger thickness.<sup>3,5,6,21,22</sup> The spin- and symmetry-projected bands for bcc Fe, bct Co, and hcp Co are presented in Fig. 1 along the related high-symmetry lines of the different BZ.<sup>23</sup> Solid (dashed) lines indicate majority- (minority-) spin character bands, and the regions below  $E_F$  are shaded. For bcc Fe and bct Co, the notation  $\Delta_1$  ( $\Delta_5$ ) refers to bands having  $m_l = 0$  ( $m_l = \pm 1$ ). The  $H$  critical points are also indicated and their energy given for both spin directions. For hcp Co the band symmetry is instead labeled by the related  $m_l$  values. The results for bcc Fe and hcp Co are in good analogy with previous calculations reported in Refs. 20, 24, and Ref. 25, respectively. A comparison between bcc Fe and bct Co shows some substantial differences in the band structure close to the  $H$  point. These are due to the mentioned crystallographic distortion of the resulting Co structure and will be shown to play a relevant role in the interpretation of our spectroscopic results.<sup>26</sup>

In Fig. 2 the AC results are given in the spin-integrated mode in the 0–50 ML Co coverage range. The spectrum of the clean Fe(001) surface, which has previously been discussed,<sup>10,27</sup> shows the typical line shape of all bcc structures due to the presence of a symmetry-related  $\Delta_1$  energy gap between the  $H_{15}$  and the  $H_{12}$  levels at  $H$  (see Fig. 1). Within this gap the impinging electrons cannot accommodate into the solid and are largely reflected, causing a deep minimum visible at  $\sim 11.5$  eV, with respect to  $E_F$ , in the AC spectrum. The sharp onset at lower energy is instead related

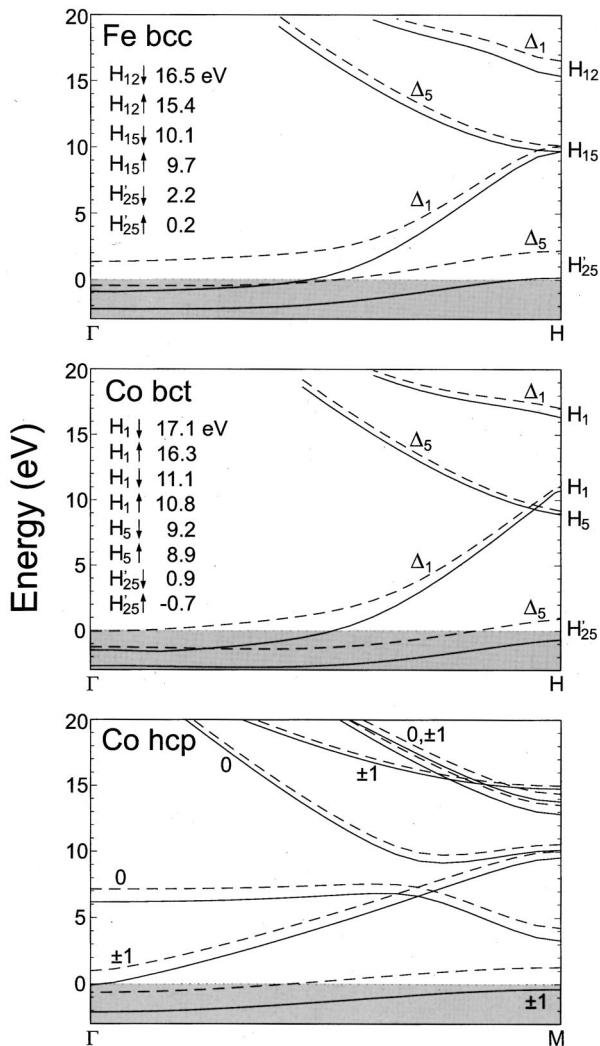


FIG. 1. Band-structure calculations for bcc Fe, bct Co, and hcp Co. Dashed (solid) lines refer to minority (majority-spin contributions). For bcc Fe and bct Co, the  $H$  critical points are shown and their energies given, where  $\uparrow(\downarrow)$  indicates majority (minority) spins;  $\Delta_1$  ( $\Delta_5$ ) bands refer to  $m_l=0$  ( $\pm 1$ ). For hcp Co bands are labeled by their  $m_l$  value. The energy zero is at  $E_F$ , and the range of occupied states is shaded.

to the crossing of the vacuum level since electrons with lower energy cannot enter the solid.

Moving to the results concerning the Co/Fe(001) interface, it is worth noting that, due to the small value [few Å (Ref. 28)] of the electron penetration depth in the energy range used here for both AC and IPE spectroscopies, already at 7 ML Co coverage the Fe substrate contribution to the signal is negligible and the results have to be interpreted as due only to the Co overlayer. The 7 ML coverage spectrum is quite similar to that of pure Fe, with still a well-pronounced minimum at  $\sim 1$  eV larger energy. This upward shift is well reproduced in the theory (Fig. 1) where a 1 eV shift is present, between bcc Fe and bct Co, in both the  $\Delta_1$  spin-projected bands of the  $H_{15}$  and  $H_1$  levels, respectively. At 14 and 21 ML Co coverage, the minimum in the AC spectra is completely washed out, indicating a structural modification taking place in the Co structure. At 50 ML Co coverage the AC line shape is strongly varied with respect to the typical bcc (or bct) profile and the deep minimum is now

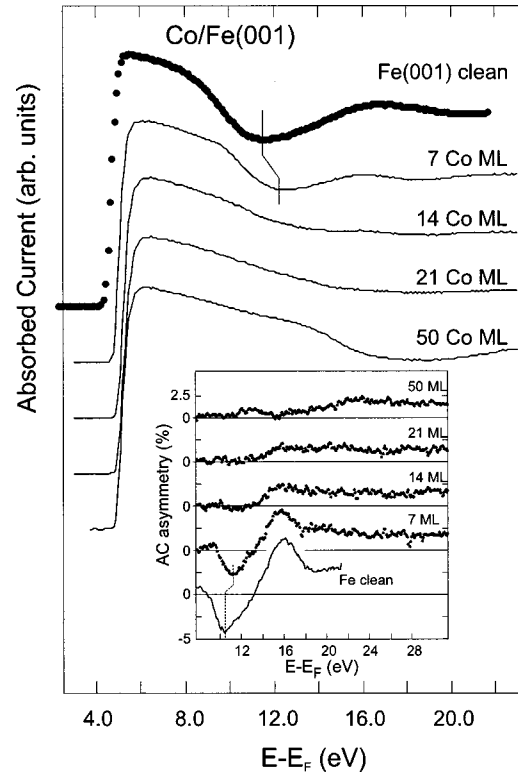


FIG. 2. AC results for the Co/Fe(001) system at various Co coverages (given in ML). Vertical bars refer to the energy range used for the subtractions made in order to evaluate the hcp character (see text). The spectrum with the shaded area is the subtraction between 50 ML Co and the clean Fe(001) profiles. Inset: related asymmetry profiles; for each spectrum, the zero-asymmetry reference is indicated by a horizontal line.

replaced by a broad and weak valley at higher energy, centered at  $\sim 20$  eV. This can hardly be related to a gap effect which, according to the calculations of Fig. 1, is not present in the hcp Co in this energy range.<sup>29</sup> A line shape analysis of the AC results in Fig. 2 shows that the bct-hcp transition occurs at  $\sim 15$  ML,<sup>22</sup> in very close agreement with previously mentioned determinations.

As mentioned above the position of the onset, with respect to  $E_F$ , in the AC spectra give a measure of the sample work function ( $\Phi$ ). In Table I the magnitude of the work function, determined by the position of the zero in the second derivative of the AC spectra of Fig. 2, is given at various Co coverages. For Fe(001) the  $\Phi$  value agrees with reported data.<sup>7,30</sup> At 7 ML Co coverage the onset moves toward higher energy, showing a trend in agreement with the larger Co work function with respect to Fe.<sup>31</sup> At 14 ML the  $\Phi$  further increases by  $\sim 0.1$  eV keeping a constant value up to the largest coverage investigated. Because of the close relationship existing between the surface structure and magnitude of the work function,<sup>32</sup> the slight increase of the Co work function occurring from 14 ML film thickness on, i.e., when hcp Co formation starts to take place, may be considered as a hint that a structural transition is occurring.

In the inset, the AC spin asymmetries ( $A$ ) are given, in percentage, for the spectra of Fig. 2.  $A$  is defined as

$$A = (I_{\uparrow} - I_{\downarrow}) / P_0(I_{\uparrow} + I_{\downarrow}),$$

TABLE I. Work function values of the Co/Fe(001) and Co/Fe(001)- $p(1 \times 1)$ O interfaces in eV at various Co coverages. The error is  $\pm 0.05$  eV.

	Co coverage (ML)							Co
	Clean	7	14	21	28	50	56	
Fe(001)	4.70	5.08	5.23	5.19		5.18		5.2 <sup>a</sup>
Fe(001)- $p(1 \times 1)$ O	4.70	4.80	4.78	4.79	4.80		4.90	

<sup>a</sup>The work function for Co refers to the Co(0001) surface as reported in Ref. 31.

where  $I_{\uparrow}$  and  $I_{\downarrow}$  represent the AC intensities for primary electrons with magnetic moment parallel and antiparallel to the sample magnetization, respectively. The oscillating behavior of  $A$  vs energy for the Fe(001) surface agrees well with previous findings and is closely related to the presence of the gap.<sup>10,33</sup> This can be understood in terms of the calculations of Fig. 1: at  $\sim 11$  eV above  $E_F$ , being across the  $H_{15}$  levels, the incoming minority-spin electrons can still be absorbed while the majority-spin electrons cannot.  $I_{\uparrow}$  is therefore smaller than  $I_{\downarrow}$ , giving rise to a negative peak asymmetry; the opposite effect is found at  $\sim 15$  eV, i.e., in the vicinity of  $H_{12}$ . As a consequence, the intensity of the asymmetry oscillation is strongly related to the value of the exchange splitting at the gap edges.

The asymmetry at 7 ML Co coverage keeps a similar profile, indicating a ferromagnetic coupling between the Co film and Fe substrate. A comparison of the spectrum with the profile of Fe(001) shows that the gap-related minimum is shifting by  $\sim 0.7$  eV toward larger energy, in analogy with the behavior of the AC spectra shown in Fig. 2. Moreover, the oscillation intensity shows a 35% decrease: this effect may be partly interpreted in terms of a reduced exchange splitting for the  $\Delta_1$  levels at both the  $H_1$  gap edges for bct Co as compared to the  $H_{15}$  and  $H_{12}$  levels of Fe(001), as suggested by calculations. A further contribution is instead related to the decreased surface order which is known to be very important in the development of spin-dependent effects.<sup>11</sup> We will further discuss this topic in Sec. IV. At 14 and 21 ML the asymmetry profiles are gradually losing the previous oscillating behavior, coherently with the mentioned absence of a gap in the hcp structure,<sup>29</sup> while a small asymmetry plateau is present at higher energy, reaching 20–25 eV at the maximum coverage investigated. This might be possibly related to the broad valley found in the AC profile and has anyway no clear counterpart in our theoretical results, as mentioned.

Figure 3 displays spin-polarized IPE results for the same set of Co coverages as for Fig. 2. The Fe(001) spectra are in nice agreement with reported results.<sup>19,34</sup> They show, in both spin channels, two peaks which have been interpreted in terms of transitions to the spin-split  $H'_{25}$  and  $H_{15}$  levels close to  $E_F$  and at  $\sim 10$  eV, respectively. This picture agrees very well with our theoretical results: the majority-spin peak related to the  $H'_{25}$  level lies just above  $E_F$ , while the minority one is found at  $\sim 2$  eV; the peaks related to the  $H_{15}$  levels are found just across the AC asymmetry minimum (see the inset of Fig. 2) and their experimental split is 0.57 eV.<sup>10</sup>

At 7 ML Co coverage the line shapes become considerably different, in the low-energy range, with respect to the

profile of Fe(001). The majority-spin spectrum is now nearly featureless, and the minority-spin profile shows an intense peak at  $\sim 0.8$  eV above  $E_F$ . On the basis of the present calculations, these results are interpreted as a global downward shift due to the filling of the related bands, which causes the majority level to move below  $E_F$ , i.e., in a region which cannot be probed by IPE. At higher energy the spectra still show the spin-split peak similar to Fe(001), but shifted by  $\sim 0.6$  eV to lower energy. Interestingly enough, the shift has an opposite sign with respect to what found, doing a similar comparison, both for the AC spectra and related spin asymmetry profiles (Fig. 2). This cannot be explained in terms of an ideal bcc Co growth since this would rather give a common downward shift for both AC and IPE results.<sup>35</sup> We therefore interpret such an effect as due to the tetragonal distortion occurring in bct Co, which is responsible for a removal of the bands degeneracy at the former  $H_{15}$  point between  $\Delta_1$  and  $\Delta_5$  symmetry levels. As a result, the  $\Delta_1$  level shifts to higher energy, while the  $\Delta_5$  level shifts to lower energy, with respect to Fe(001), as shown by calculations. The opposite shifts observed between AC and IPE spectroscopies, comparing the profiles of the Fe(001) surface with those of the 7 ML Co, give therefore a clear indication of a distorted cubic Co growth on the Fe(001) in this coverage range.

At larger Co coverages the low-energy IPE peak keeps a completely minority-spin character and the high-energy fea-

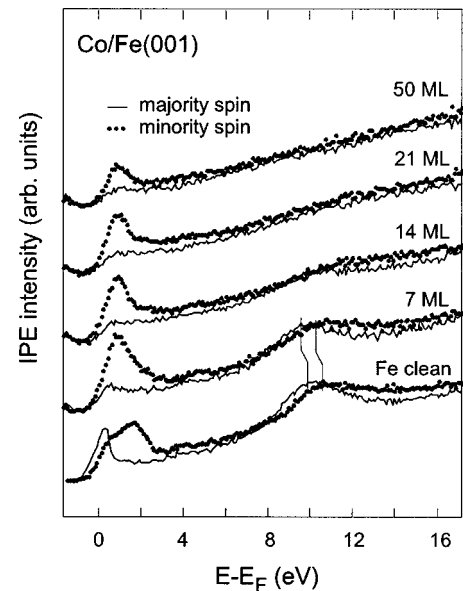


FIG. 3. Spin-resolved IPE results for the Co/Fe(001) system.

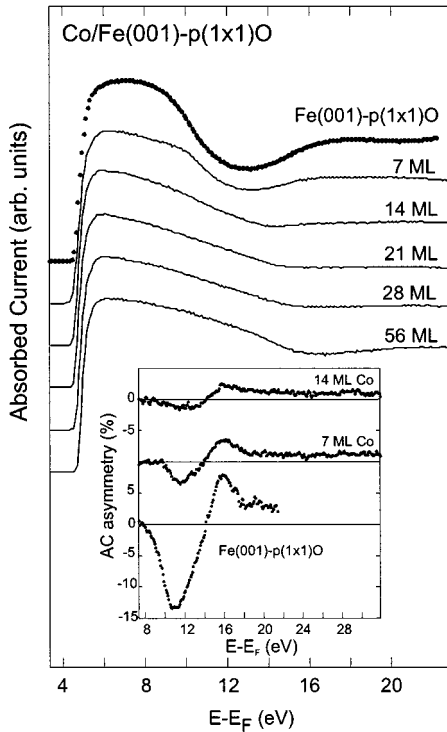


FIG. 4. AC results for the Co/Fe(001)- $p(1 \times 1)$ O system as a function of Co coverage. Inset: related asymmetry profiles; for each spectrum, the zero-asymmetry reference is indicated by a horizontal line.

tures disappear from the spectra. For a comparison of these results with hcp Co calculations, it is worth keeping in mind that, beside symmetry considerations on the  $m_l$  quantum number, also angular momentum conservation, via the  $\Delta l = \pm 1$  selection rule, and energy conservation are relevant in selecting the allowed transitions in IPE, where the detected photon energy is kept fixed. These further constrictions rule out many of the decay channels, leaving only with the minority feature clearly visible close to  $E_F$ .<sup>23</sup> This is related to a  $m_l = \pm 1$  final state having its majority counterpart lying below  $E_F$  in the calculations, similar to the case of bct Co. Furthermore, in consideration of the large amount of disorder at the surface for large thickness films, the spectral features may generally become broader and less intense. As a result, other possible higher-energy transitions might be lost inside the background in the experiments.

#### IV. Co ON Fe(001)- $p(1 \times 1)$ O

The stability range of the Co bct phase is considerably extended when the growth is performed onto the Fe(001)- $p(1 \times 1)$ O surface, due to the oxygen surfactant action which makes an oxygen monolayer to float on top of the Co surface.<sup>5,22</sup> In Fig. 4 the AC spectra for Co on Fe(001)- $p(1 \times 1)$ O are shown for various coverages. The starting substrate AC spectrum is quite similar to that of Fe(001) (see Fig. 2) with a deep minimum and agrees well with previously reported data.<sup>10</sup> Structural disorder may cause a partial relaxation of the symmetry rules given above, with relevant consequences since the typical bcc (or bct) symmetry gap is in general absent along other directions in the BZ. For systems with a similar magnitude of the gap, we

can therefore relate the depth of the minimum, normalized to the intensity maximum occurring just above threshold, to the degree of surface order. In the AC spectrum of Fe(001)- $p(1 \times 1)$ O, this is 30% larger (i.e., more pronounced) than for the AC profile of Fe(001), indicating that the surface order is improved by the oxygen surfactant action. As for the 7 ML Co film, the depth of the minimum is now  $\sim 10\%$  larger than that of the spectrum referring to the same coverage onto Fe(001). Though smaller than above, the effect is qualitatively interpreted in terms of a better ordered Co overlayer growing on Fe(001)- $p(1 \times 1)$ O, similarly to the case of Fe homoepitaxy<sup>11</sup> on this substrate. Increasing the Co coverage, one obtains a less and less pronounced minimum shifting toward larger energy. The shift is caused by the gradually reduced intensity of the minimum which sits on top of a strongly decreasing profile vs energy. At 28 ML the minimum is no longer present and a plateau takes place in the range 15–22 eV. This evolution seems to imply a slower dynamics if compared to the results of Co/Fe(001) where already at 14 ML Co coverage the gap-related minimum has completely disappeared. At 56 ML the profile starts to show a new higher-energy minimum. In agreement with the previous picture, this can be interpreted as a precursor feature evolving toward the hcp-like line shape displayed by the 50 ML Co coverage on Fe(001), as shown in Fig. 2. A line shape analysis of the AC results in Fig. 4 shows that the bct-hcp transition occurs now at  $\sim 35$  ML.<sup>22</sup> This value is more than twice the one found for the Co growth on Fe(001), giving a confirmation of the above mentioned picture.

As reported in Table I, the study of the work function for various Co coverages does not give, in this case, a clear trend at variance with the Co/Fe(001) growth. For the Fe(001)- $p(1 \times 1)$ O structure, we find the same  $\Phi$  as for the clean Fe(001) surface, in agreement with previous estimations.<sup>7,10,30</sup> At all Co coverages here investigated, the work function keeps basically constant at  $\sim 4.8$ – $4.9$  eV. This value is considerably smaller than what we found for any Co coverage on Fe(001). Due to the mentioned surface segregation of oxygen in this interface, the topmost layer has to be regarded as a Co surface oxide instead of a pure Co surface. This may likely pin the work function to the value of the related Co surface oxide irrespective of the underlying Co crystal symmetry, therefore preventing one from following structural transition. This argument is supported by a recent study of the work function variation upon oxidation of the Co(11 $\bar{2}$ 0) surface.<sup>36</sup> It is there shown that for an oxygen overlayer thickness of  $\sim 1$  ML, i.e., similar to our case, the work function decreases by 0.3–0.4 eV with respect to the clean Co surface, in very nice agreement with our comparison between the results for 50 ML Co/Fe(001) and for 50 ML Co/Fe(001)- $p(1 \times 1)$ O 56 ML Co/Fe(001)- $p(1 \times 1)$ O.

In the inset the spin asymmetries for the AC spectra of Fig. 5 are reported. The large intensity oscillation shown by the Fe(001)- $p(1 \times 1)$ O profile, which is more than double if compared to that of Fe(001), is one of the enhanced spin-dependent effects displayed by the oxidized phase.<sup>10</sup> When 7 ML Co are grown on top of it, the magnitude of the asymmetry clearly decreases. Nevertheless, the oscillation is 20% larger than that of the 7 ML coverage on Fe(001) (cf. Fig. 2). The increased magnitude of spin-dependent effects shown by the bct Co grown on Fe(001)- $p(1 \times 1)$ O is similar to what

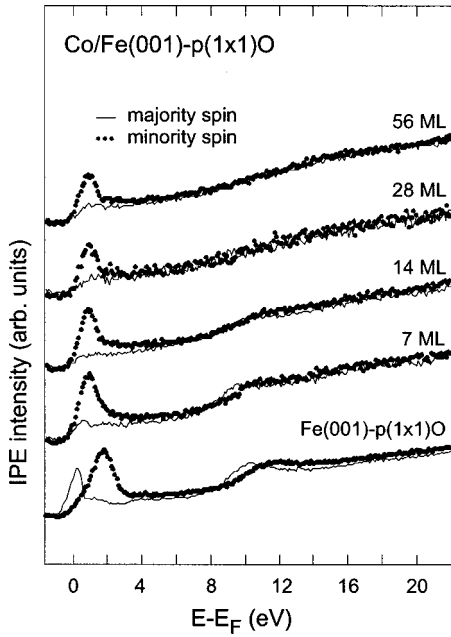


FIG. 5. Spin-resolved IPE results for the Co/Fe(001)- $p(1 \times 1)$ O system.

reported for Fe(001)- $p(1 \times 1)$ O as compared to Fe(001) and puts in evidence the role played by oxygen on the magnetic properties as well. The same trend is found when comparing the results of the 14 ML coverages on the two substrates. At higher Co thickness the asymmetry gradually disappears.

Figure 5 shows the IPE results for this interface. The Fe(001)- $p(1 \times 1)$ O spectrum, in agreement with previous results,<sup>10,37</sup> resembles the Fe(001) IPE profile, although the effect of larger spin-dependent effects is evidenced in the considerably larger splitting of the  $H_{15}$  levels around 10 eV: this is now 0.87 eV as compared to 0.57 for Fe(001).<sup>10</sup> In the 7 ML coverage spectrum, the majority-spin contribution close to  $E_F$  is absent and the minority one shifts to lower energy at  $\sim 0.8$  eV, similar to the profile of the same coverage on Fe(001). The high-energy feature shows the same splitting as that of 7 ML Co on Fe(001), while the energy scale shifts upward by  $\sim 0.2$  eV in analogy to AC results for this coverage. At 14 ML these states are still barely visible, at variance with the case of the same coverage on Fe(001) where they have already vanished, confirming that surface order of the Co overlayer is better achieved, for a given coverage, on Fe(001)- $p(1 \times 1)$ O than on Fe(001). For higher coverages IPE spectra do not show any further evolution, as expected considering the results for the Co/Fe(001) system.

## V. FeCo COMPOUND FORMATION AND SURFACE OXIDATION

The Fe-Co phase diagram shows the occurrence of a few stable bcc substitutional compounds<sup>38</sup> which display interesting magnetic properties.<sup>39</sup> In order to investigate their possible formation as a product of the Co/Fe(001) interfacing, we have thermally treated this system. After evaporating a 21-ML-thick Co overlayer keeping the Fe substrate at room temperature, an annealing at 900 K has been carried out for 5 min. A clear  $(1 \times 1)$  LEED pattern is obtained. An XPS

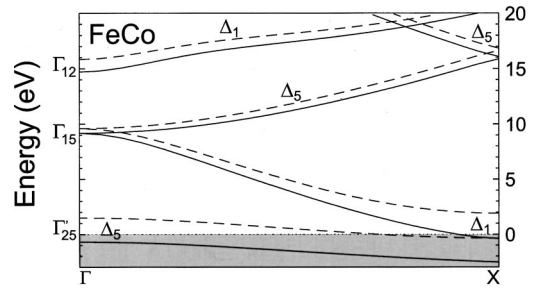


FIG. 6. Band-structure calculations for the simple cubic structure of FeCo. Dashed (solid) lines refer to minority-(majority-) spin contributions.  $\Delta_1$  ( $\Delta_5$ ) bands refer to  $m_l=0$  ( $\pm 1$ ). We have omitted, for the sake of clarity, a  $\Delta_1$  band lying completely below the vacuum level (see Ref. 23). The  $\Gamma$  critical points are indicated, and their energies are the following, with the same notation used in Fig. 2:  $\Gamma_{12}\downarrow 15.8$  eV,  $\Gamma_{12}\uparrow 14.7$  eV,  $\Gamma_{15}\downarrow 9.6$  eV,  $\Gamma_{15}\uparrow 9.2$  eV,  $\Gamma'_{25}\downarrow 1.5$  eV, and  $\Gamma'_{25}\uparrow -0.7$  eV.

intensity analysis based on the Fe and Co  $2p_{3/2}$  core level peaks indicates the formation of a compound with FeCo stoichiometry. This has been subsequently oxidized at the surface with the same procedure reported in Sec. II for obtaining the Fe(001)- $p(1 \times 1)$ O surface. After this operation LEED results show a sharp  $(1 \times 1)$  pattern and the XPS analysis indicates that an oxygen monolayer forms at the surface.

FPLO calculations have been performed for FeCo, which has the CsCl simple cubic structure with a 1.41 Å lattice spacing.<sup>38</sup> This makes a good matching with the Fe substrate, ruling out any sizable stress in the FeCo crystal. Following the same geometry argument given in Sec. II, the states accessible to our AC and IPE experiments for the simple cubic (sc) crystal of FeCo(001) lie along the  $\Gamma X$  direction, which exhibits  $\Delta$ -like symmetry bands. They are shown in Fig. 6, with the same meaning of the symbols as in Fig. 1. The sc band structure along  $\Gamma X$  can be viewed<sup>38</sup> as the folding of a bcc band structure midway along  $\Gamma H$  in such a way to overlap the  $H$  point with the BZ center. In this band structure the minimum of the  $\Delta_1$  energy gap is thus located at  $\Gamma$ . The energies of the  $\Gamma$  critical points are given in the figure caption.

In Fig. 7 the AC spectra of the FeCo, before and after the oxidation process described above, are shown. For FeCo a clear gap-related minimum is present coherently with the results of the band-structure calculations. The spectrum is quite similar to the Fe(001) profile including the position of the onset which gives for FeCo a work function of 4.75 eV. After oxidation, the profile keeps a similar shape, showing a 30% more pronounced minimum. In analogy to the case of Fe(001) oxidation, this indicates that the oxygen surfactant action plays a sizable ordering role in this case as well.

The asymmetry spectra associated to the above AC results are shown in the inset of Fig. 7. FeCo(001) and Fe(001) profiles are similar to each other in terms of the oscillation intensity, in agreement with our calculations, which basically give the same values of the exchange splitting for the pure Fe and for the compound. The FeCo spectrum is slightly shifted to larger energy by  $\sim 0.1$ – $0.2$  eV, in qualitative agreement with theoretical findings which actually give a  $\sim 0.6$ – $0.7$  eV

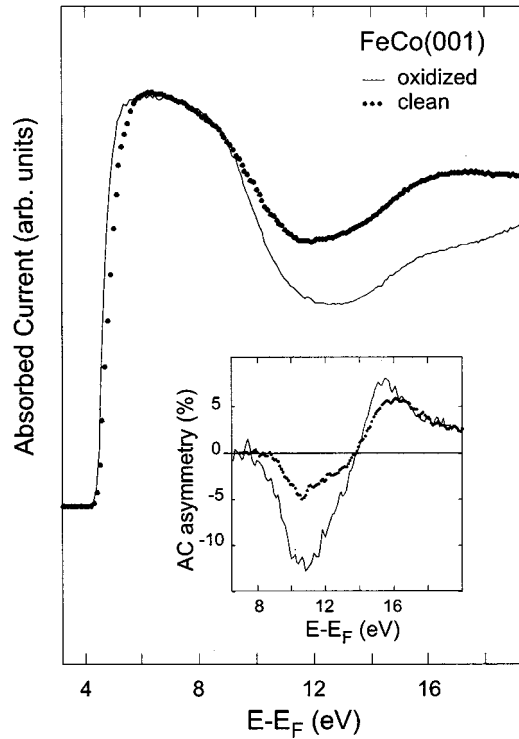


FIG. 7. AC results for the FeCo compound before and after the surface oxidation process (see text). Inset: related asymmetry profiles.

shift on both sides of the gap, keeping the same gap amplitude. Upon oxidation, a strong enhancement of the asymmetry is visible and this reaches the large values found for the Fe(001)- $p(1 \times 1)$ O, as shown in Fig. 4. Thus, for the oxidation of FeCo, the mechanism leading to the increase of spin-dependent effects seems to be basically the same as for the case of Fe(001)- $p(1 \times 1)$ O, given in Ref. 9. Following this interpretation, the surface magnetism enhancement can be qualitatively interpreted in terms of the giant adsorption-induced relaxation occurring at the oxidized surface. This gives rise to a metal-metal bond length at the surface larger than in the bulk, with an increase of the magnetic moments towards the value of isolated atoms.

In Fig. 8 IPE spectra are presented. For FeCo close to  $E_F$  a strong minority feature is visible, while in the majority-spin profile only a small shoulder, if any, is present coherently with the theoretical results of Fig. 6, which predict the majority states to lie 0.7 eV below  $E_F$ . It is interesting to note that, at variance with the work function value which is very close to the Fe limit, the IPE profiles have a strong Co-like character. In fact, in both calculations and experiments Fe presents a majority-spin contribution just above  $E_F$ , while in Co this has shifted below  $E_F$ . The position of the minority-spin feature is  $\sim 1.3$  eV above  $E_F$ , i.e., a value between the 0.8 eV found for both bct and hcp Co and the 2 eV of Fe(001) as expected on the basis of a band filling effect. At higher energy the peak related to the lower edge of the symmetry gap is clearly visible on both spin channels: the splitting is the same as for Fe(001), while a small upward shift is visible. These results agree with both the experimental findings on the asymmetry profiles and the calculations. Upon oxidation, the spectra keep a similar shape, but the exchange splitting at  $\sim 10$  eV has now increased to

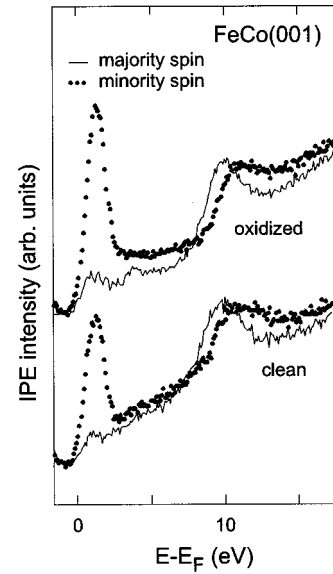


FIG. 8. Spin-resolved IPE results for the FeCo compound before and after the surface oxidation process.

$\sim 0.85$  eV which is the same value found for Fe(001)- $p(1 \times 1)$ O. These results are coherent with the above picture about the role of oxygen for increasing the surface magnetic effects on the FeCo compound as well.

## VI. CONCLUSIONS

We have presented a combined experimental and theoretical study of the Co growth as a thin film onto the Fe(001) surface in different growing regimes including the role of oxygen in modifying the properties of the Co growth. Fe-Co represents an interesting system, both from basic and technological research, due to the strong magnetic character of the species involved. First-principles calculations have been performed by means of an updated version of the original FPLO scheme, giving particular emphasis on the empty state region above  $E_F$ . Experiments, in fact, have probed these states by means of spin-resolved AC and IPE spectroscopies, giving therefore access to structural, electronic, and magnetic information about this system. Nice agreement has generally been found between theory and experiments. As for the Co/Fe(001) interface, an initial Co distorted cubic growth (bct) has been found, up to about 15 ML, with respect to the bcc structure of the substrate. At larger coverages Co grows in its equilibrium hcp structure. In both cases we found a ferromagnetic coupling between the overlayer atoms and substrate. The Co/Fe(001)- $p(1 \times 1)$ O interface shows a behavior qualitatively similar to Co/Fe(001), but the range of stability of the bct Co structure is now extended up to about 35 ML. Furthermore, a surfactant action of oxygen is present, giving rise to an increased surface order and enhanced spin-dependent effects with respect to Co/Fe(001). Our work function study supports this interpretation. The third situation studied is represented by the formation of a stoichiometric cubic FeCo(001) compound upon thermal treatment of the Co/Fe(001) interface. The trends shown are understood in terms of a progressive band filling on going from Fe to FeCo to Co. The FeCo surface oxidation shows an en-

hancement of the spin-dependent effects similar to the surface oxidation of pure Fe(001).

#### ACKNOWLEDGMENTS

This work has been supported by the Italian Ministry of University and Scientific and Technological Research

through the MURST-Cofin99 Project No. 9902118418-003. One of us (M.R.) would like to thank K. Koepernik, H. Eschrig, and I. Opahle for their allowance and help in using the FPLO code. Further, he is grateful to the Bundesministerium für Bildung und Forschung der BRD for financial support (Project No. 13N7443/1).

- <sup>1</sup>*Ultrathin Magnetic Structures*, edited by B. Heinrich and J. A. Bland (Springer-Verlag, Berlin, 1994), Vols. I and II.
- <sup>2</sup>G. A. Prinz, in *Ultrathin Magnetic Structures* (Ref. 1), Vol. II, p. 1; G. A. Prinz, E. Kisker, K. B. Hathaway, K. Schröder, and K.-H. Walker, *J. Appl. Phys.* **57**, 3024 (1985).
- <sup>3</sup>Hong Li and B. P. Tonner, *Phys. Rev. B* **40**, 10 241 (1989).
- <sup>4</sup>D. Pescia, G. Zampieri, M. Stampanoni, G. L. Bona, R. F. Willis, and F. Meier, *Phys. Rev. Lett.* **58**, 933 (1987); C. M. Schneider, P. Bresseler, P. Schuster, J. Kirschner, J. J. de Miguel, and R. Miranda, *ibid.* **64**, 1059 (1990); A. Clarke, G. Jennings, R. F. Willis, P. J. Rous, and J. B. Pendry, *Surf. Sci.* **187**, 327 (1987).
- <sup>5</sup>S. K. Kim, C. Petersen, F. Jona, and P. M. Marcus, *Phys. Rev. B* **54**, 2184 (1996).
- <sup>6</sup>G. C. Gazzadi and S. Valeri, *Europhys. Lett.* **45**, 501 (1999).
- <sup>7</sup>C. F. Brucker and T. N. Rhodin, *Surf. Sci.* **57**, 523 (1976).
- <sup>8</sup>K. O. Legg, F. Jona, D. W. Jepsen, and P. M. Marcus, *Phys. Rev. B* **16**, 5721 (1977).
- <sup>9</sup>S. R. Chubb and W. E. Pickett, *Phys. Rev. Lett.* **58**, 1248 (1987); *Solid State Commun.* **62**, 19 (1987); *Phys. Rev. B* **38**, 10 227 (1988).
- <sup>10</sup>R. Bertacco and F. Ciccacci, *Phys. Rev. B* **59**, 4207 (1999).
- <sup>11</sup>F. Bisio, R. Moroni, M. Canepa, L. Mattera, R. Bertacco, and F. Ciccacci, *Phys. Rev. Lett.* **83**, 4868 (1999).
- <sup>12</sup>K. Koepernik and H. Eschrig, *Phys. Rev. B* **59**, 1743 (1999).
- <sup>13</sup>F. Ciccacci, E. Vescovo, G. Chiaia, S. De Rossi, and M. Tosca, *Rev. Sci. Instrum.* **63**, 3333 (1992); G. Chiaia, S. De Rossi, L. Mazzolari, and F. Ciccacci, *Phys. Rev. B* **48**, 11 298 (1993).
- <sup>14</sup>R. Bertacco, S. De Rossi, and F. Ciccacci, *J. Vac. Sci. Technol. A* **16**, 2277 (1998).
- <sup>15</sup>R. Bertacco, M. Merano, and F. Ciccacci, *Appl. Phys. Lett.* **72**, 2050 (1998).
- <sup>16</sup>J. B. Benziger and R. Madix, *J. Electron Spectrosc. Relat. Phenom.* **20**, 281 (1980).
- <sup>17</sup>F. Ciccacci, S. De Rossi, and D. M. Campbell, *Rev. Sci. Instrum.* **66**, 4161 (1995).
- <sup>18</sup>I. Opahle, K. Koepernik, and H. Eschrig (unpublished).
- <sup>19</sup>A. Santoni and F. J. Himpsel, *Phys. Rev. B* **43**, 1305 (1991).
- <sup>20</sup>E. Tamura, R. Feder, J. Krewer, R. E. Kirby, E. Kisker, E. L. Garwin, and F. K. King, *Solid State Commun.* **55**, 543 (1985).
- <sup>21</sup>J. Dekoster, E. Jedryka, C. Mény, and G. Langouche, *Europhys. Lett.* **22**, 433 (1993).
- <sup>22</sup>R. Bertacco, G. Isella, L. Duò, F. Ciccacci, A. di Bona, P. Luches, and S. Valeri, *Surf. Sci.* (to be published).
- <sup>23</sup>The weight of the proper  $m_l$  contributions is always unit apart from the  $m_l = \pm 1$  case in the hcp structure, where the weight is fractional and always  $>0.6$ . Since we will not make here definite statements on the intensities of the IPE features, we can safely neglect this effect. Furthermore, on the basis of the argument given in Sec. II concerning the small IPE detection probability for  $m_l=0$  final states, in the hcp band structure of Fig. 1 we have omitted, for the sake of clarity, those  $m_l=0$  symmetry bands which lie completely below the vacuum level. In fact, they are not detected in AC or in IPE spectroscopies as will be shown below.
- <sup>24</sup>E. Tamura and R. Feder, *Phys. Rev. Lett.* **57**, 759 (1986).
- <sup>25</sup>D. A. Papaconstantopoulos, *Handbook of the Band Structure of Elemental Solids* (Plenum, New York, 1986).
- <sup>26</sup>We will instead neglect, at this stage, possible effects due to the smaller lattice distortion in the hcp growth of Co at large thickness with respect to the ideal hcp Co crystal.
- <sup>27</sup>F. Ciccacci and S. De Rossi, *Phys. Rev. B* **51**, 11 538 (1995).
- <sup>28</sup>D. P. Pappas, K.-P. Kämper, B. P. Miller, H. Hopster, D. E. Flower, C. R. Brundle, A. C. Luntz, and Z.-X. Shen, *Phys. Rev. Lett.* **66**, 504 (1991); Schönense and H. C. Siegmann, *Ann. Phys. (Leipzig)* **2**, 465 (1993).
- <sup>29</sup>A narrow gap is in fact present in the hcp calculations at much smaller energy ( $\sim 7$  eV), but it is not present in the AC spectrum.
- <sup>30</sup>K. Ueda and R. Shimizu, *Jpn. J. Appl. Phys.* **11**, 916 (1972); Y. Sakisaka, T. Miyano, and M. Onchi, *Phys. Rev. B* **30**, 6849 (1984).
- <sup>31</sup>F. J. Himpsel, *Phys. Rev. B* **43**, 13 394 (1991).
- <sup>32</sup>J. Hölzl and F. K. Schulte, in *Work Function of Metals*, Springer Tracts in Modern Physics Vol. 85, edited by G. Höhler and E. A. Niekisch (Springer-Verlag, Berlin, 1979), p. 1.
- <sup>33</sup>Th. Dotd, D. Tillmann, R. Rochow, and E. Kisker, *Europhys. Lett.* **6**, 375 (1988).
- <sup>34</sup>J. Kirschner, M. Glöbl, V. Dose, and H. Scheidt, *Phys. Rev. Lett.* **53**, 612 (1984); S. De Rossi and F. Ciccacci, *J. Electron Spectrosc. Relat. Phenom.* **76**, 177 (1995).
- <sup>35</sup>This is what results from our calculations on ideal bcc Co, which have not been shown here.
- <sup>36</sup>B. Klingenberg, F. Grellner, D. Borgmann, and G. Wedler, *Surf. Sci.* **383**, 13 (1997).
- <sup>37</sup>S. De Rossi, L. Duò, and F. Ciccacci, *Europhys. Lett.* **32**, 687 (1995).
- <sup>38</sup>K. Schwarz, P. Mohn, P. Blaha, and J. Kübler, *J. Phys. F: Met. Phys.* **14**, 2659 (1984).
- <sup>39</sup>M. F. Collins and J. B. Forsyth, *Philos. Mag.* **8**, 401 (1963); S. Spooner, J. W. Lynn, and J. W. Cable, in *Magnetism and Magnetic Materials*, edited by D. C. Graham, and J. J. Rhyne, AIP Conf. Proc. No. 5 (AIP, New York, 1971), p. 1415.